Fractals, Vol. 7, No. 2 (1999) 133–138

TIME-DELAY EMBEDDINGS OF IFS ATTRACTORS

SONYA BAHAR*
Department of Physics and Center for Nonlinear and Complex Systems, Duke University, Box 90305, Durham, North Carolina 27708 USA

Received January 19, 1999; Accepted February 10, 1999

Abstract

A modified type of iterated function system (IFS) has recently been shown to generate images qualitatively similar to "classical" chaotic attractors. Here, we use time-delay embedding reconstructions of time-series from this system to generate three-dimentional projections of IFS attractors. These reconstructions may be used to access the topological structure of the periodic orbits embedded within the attractor. This topological characterization suggests an approach by which a rigorous comparison of IFS attractors and classical chaotic systems may be attained.

A modified iterated function system (IFS) has recently been shown to generate images resembling the classical chaotic attractors generated by nonlinear dynamical systems. These "IFS attractors" exhibit dynamical structure and are classifiable by symbolic dynamics.[1] In the present paper, we illustrate how their three-dimensional structures may be accessed by a time-delay embedding reconstruction.

A typical IFS consists of N affine transformations of the form

$$\begin{aligned} x_{n+1} &= a_i x_n + b_i y_n + c_i \\ y_{n+1} &= d_i x_n + e_i y_n + f_i \end{aligned} \tag{1}$$

where $i = 1, \ldots, N$, and a_i, b_i, c_i, d_i, e_i and f_i are constants, and each transformation is assigned a probability p_i. A fractal image is generated from an IFS by iterating the mapping according to the scheme described by Barnsley[2] in which each new point is generated from the previous point by the application of one of the N transformations. The particular transformation to be employed in each transformation is selected at random, with probability p_i.

An IFS attractor is generated by a similar algorithm, except that in place of the affine transformations in (1), we have

*E-mail: bahar@phy.duke.edu

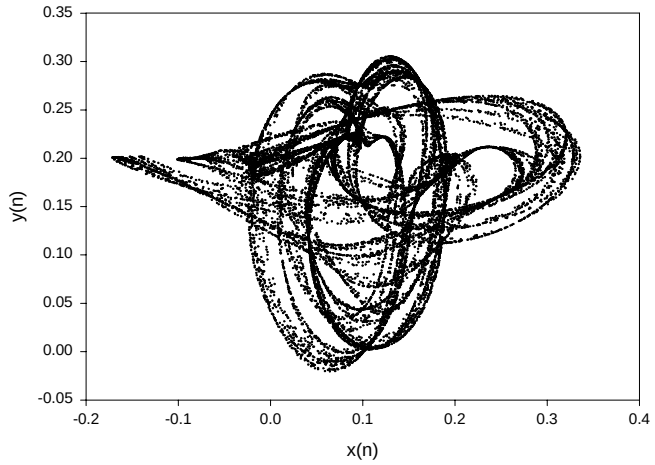

Fig. 1 Projection on the xy plane of an IFS attractor generated by iterating two transformations of the form Eq. (2). Parameters are $s_x = 0.3$, $s_y = 0.45$, $\omega_x = \omega_y = 0.49$, $a_1 = 0.7$, $b_1 = 0.9$, $c_1 = 0.1$, $d_1 = 1$, $e_1 = 1$, $f_1 = 0.2$, $a_2 = 1$, $b_2 = 2.5$, $c_2 = 0.1$, $d_2 = 1$, $e_2 = -1$ and $f_2 = 0.2$. The two transformations have equal probability ($p_1 = p_2 = 0.5$). The figure shows the results of 20 000 successive iterations (with the first 100 transient points deleted). Initial points for the first iteration were $x(0) = y(0) = 100$.

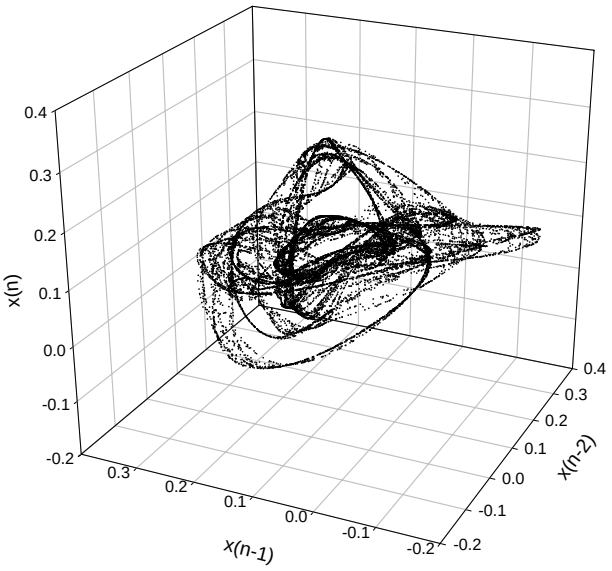

Fig. 2 Three-dimensional time-delay reconstruction of the x-data time-series of Fig. 1; x_{n-2} is plotted versus x_{n-1} and x_n. Parameters are the same as in Fig. 1; 20 000 points are shown, with the exception of the initial 100 points discarded as transients.

$$\begin{aligned} x_{n+1} &= s_x \sin(n/\omega_x)(a_i x_n + b_i y_n) + c_i \\ y_{n+1} &= s_y \cos(n/\omega_y)(d_i x_n + e_i y_n) + f_i \,. \end{aligned} \tag{2}$$

Typically we set $N = 2$, with each of the transformations assigned an equal probability ($p_i = 0.5$, $i = 1, 2$). For convenience of notation, we refer to the transformation where $i = 1$ as transformation A, and the transformation where $i = 2$ as transformation B. One of the remarkable aspects of the two-dimensional objects generated by such transformations is that they "appear" to be a projection of a three-dimensional attractor onto the xy plane (Fig. 1). The stretching and folding inherent in the classical attractors of nonlinear dynamics is plainly visible to the eye, but is it actually there? Are IFS attractors really dynamical creatures, possessed of a topological structure in the same sense as, say, the Rossler band or the BZ attractor?

It has recently been shown by Stark et al.[3] that the Takens embedding theorem can be extended to deterministic systems driven by stochastic processes. With this result as a motivation, we consider whether it is possible to treat the points generated from (2) as a time-series and to re-embedd them in a space of higher dimension than the xy plane. Consider a time-delay embedding where $(x_{n-2}, x_{n-1}, x_n) \to (x, y, z)$. Using this reconstruction on a time-series generated from (2), we obtain the image shown in Fig. 2, a three-dimensional reconstruction of the xy plane image shown in Fig. 1. A different reconstruction may be obtained by performing the partial embedding $(x_{n-1}, y_{n-1}, x_n) \to (x, y, z)$, shown in Fig. 3.

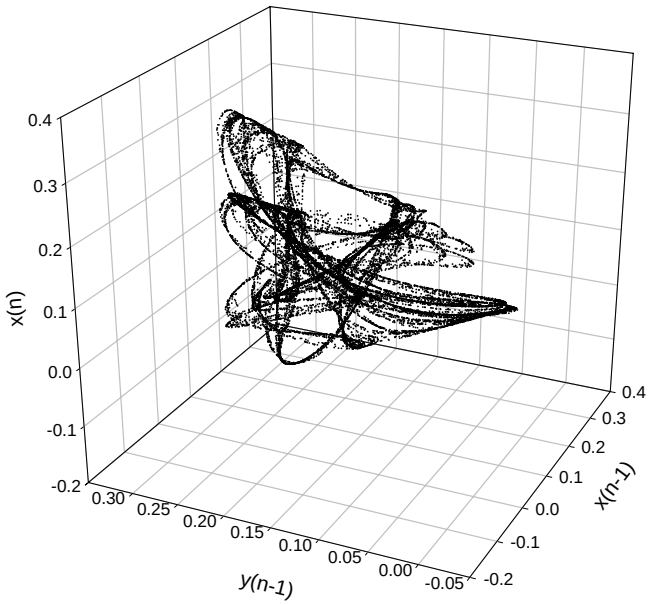

Fig. 3 Partial time-delay reconstruction of data from Fig. 1; x_{n-1} is plotted versus y_{n-1} and x_n.

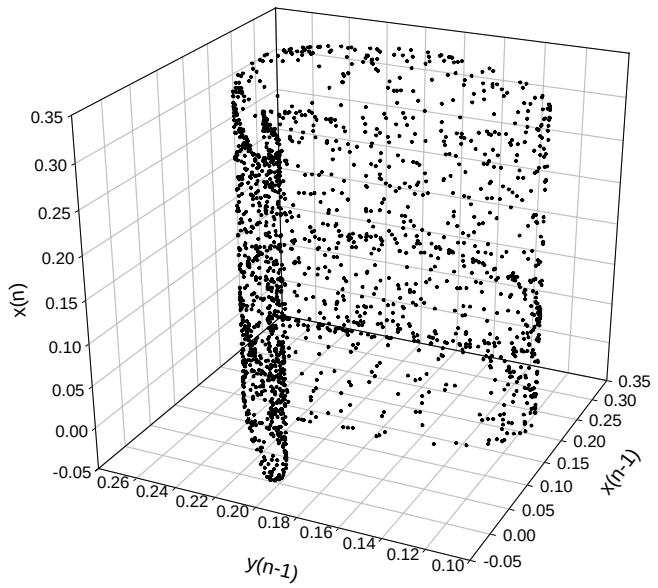

Fig. 4 Partial time-delay reconstruction of an "embedded orbit" (of sequence ...AAAAABAB, using a notation in which the most recent transformation is shown at the right) from the attractor shown in Figs. 1–3. The sequence occurs 1941 times over 499 000 iterations.

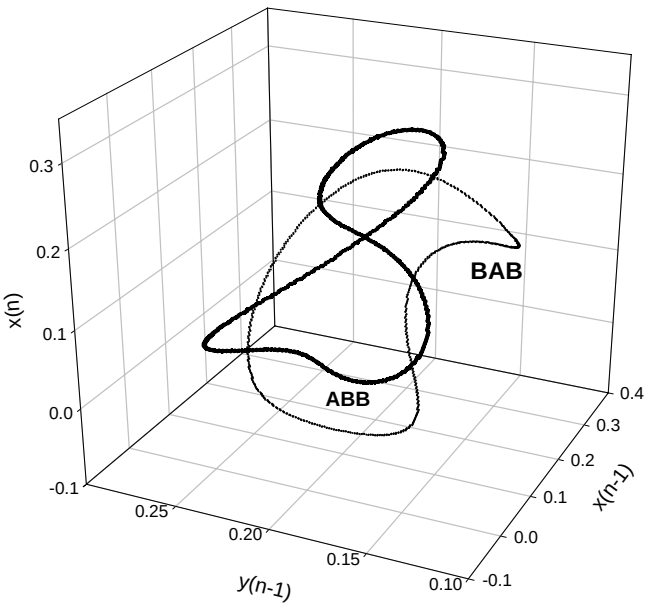

Fig. 5 Partial time-delay reconstruction of "ordered orbits" generated from the attractor shown in Figs. 1–3. The orbits are generated by transformation sequences ABB (thick curve) and BAB (thin curve).

Can we extract actual dynamics from the images shown in Fig. 2 or Fig. 3? Since IFS attractors are generated by a random accretion of points within an overall deterministic structure, we cannot extract embedded orbits from Figs. 2 or 3 as we could with a time-series generated by numerically integrating a set of nonlinear dynamical differential equations, or from a sequentially sampled set of experimentally measured values from a chaotic system. The images in Figs. 1, 2 and 3 correspond to random samplings of a time-series. Despite this limitation, however, two different types of "orbits" have been found to be associated with IFS attractors. "Embedded orbits," quite different from those extracted from classical nonlinear dynamical systems, have been found by sampling points from the IFS attractor each time a particular sequence of transformations occurs in the random generating sequence which drives the IFS.[4] Such embedded orbits appear to lie within the attractor when viewed in the xy plane.[4] However, a partial reconstruction of such an embedded orbit, shown in Fig. 4, shows a decorrelated cluster of points, since a sequence of transformations of varying length intervenes between each sampled point. (Note that some structure is evident in Fig. 4, i.e. the points are not totally decorrelated. This results from the fact that we show only a partial embedding, hence some of the structure of the original xy plane image is retained. A full embedding, $(x_{n-2}, x_{n-1}, x_n) \rightarrow (x, y, z)$, would show a totally unstructured cluster of dots.)

A more promising approach is provided by considering "ordered algorithm" orbits,[5] generated by a repeated deterministic sequence of the transformations given in (2), with a point plotted after each repeat of the sequence of transformations. Time-delay embeddings of ordered algorithm orbits retain their structure, as shown in Fig. 5. These orbits are quite different from unstable orbits in classical chaotic systems, but they may still provide a basis for a preliminary topological investigation of IFS attractors, as we shall see.

Topological studies of unstable orbits have provided much insight into the structure of chaotic attractors. The invariant topological properties of a chaotic system may be characterized by the linking numbers of unstable periodic orbits embedded in an attractor.[6–9] These linking numbers provide a "template" for the stretching and folding within the attractor and allow comparison of the topological properties among various low-dimensional dynamical systems. With the three-dimensional reconstruction of ordered orbits associated with IFS attractors, we may construct an analogous topological characterization.

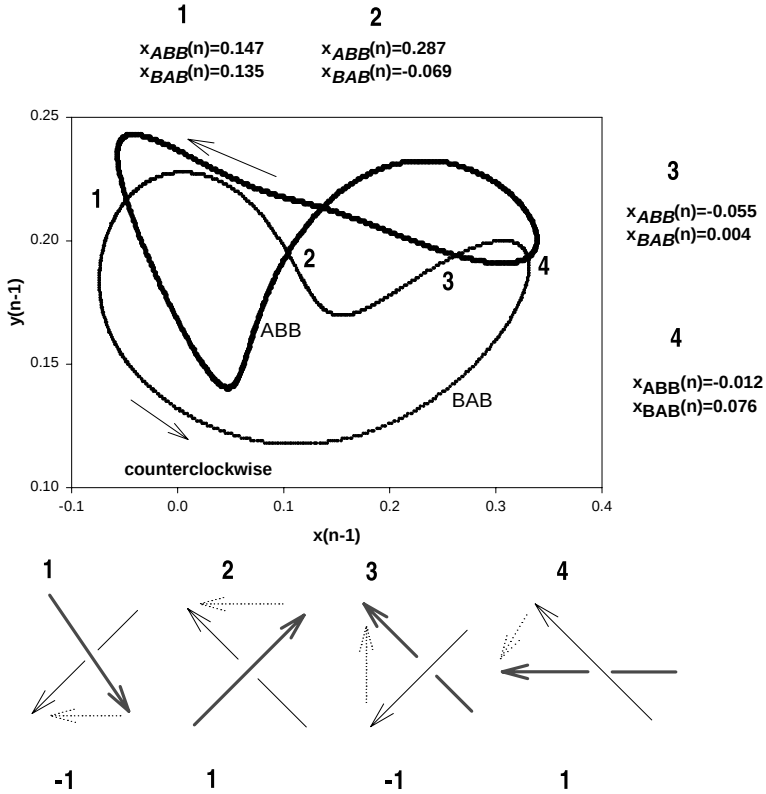

Fig. 6 How to determine linking numbers. The two ordered orbits shown in Fig. 5 are projected onto the $x_{n-1}y_{n-1}$ plane. The x_n coordinate of each of their four crossings in this plane of projection are shown. At each crossing, tangents are drawn to the orbits, pointing in the "direction of flow," which we have arbitrarily defined as counterclockwise. These tangents are indicated by the arrow pairs at the bottom of the figure. Thick arrows correspond to tangents of ABB, and thin arrows correspond to tangents of BAB. The tangent to the orbit which lies "above" in the x_n direction (perpendicular to the page) is rotated toward the tangent to the orbit lying "below," as indicated by the dotted arrows, through the smallest angle. If this rotation is counterclockwise, the crossing is assigned a value of $+1$, and if the rotation is clockwise, the crossing is assigned a value of -1. Half the sum of the signed crossings gives the "linking number" of the orbits; in the particular example shown here L(ABB, BAB) = 0.

The linking numbers of two orbits in a three-dimensional space are determined as illustrated in Fig. 6. The two orbits are projected onto a two-dimensional plane (in this case, x_{n-1} versus y_{n-1}). At each point where the projections cross in the plane, tangent vectors to each orbit are drawn in the direction of flow. Now we consider the direction perpendicular to the plane of projection (in this case, the direction along the x_n axis). At each crossing point, the tangent vector of the orbit lying "above" in this perpendicular direction is rotated toward the tangent vector of the orbit lying "below," through the smallest angle. If the rotation is counterclockwise, the crossing is assigned a value of 1, and if the rotation is clockwise, the crossing is assigned a value -1. The same procedure is followed at each intersection of the orbits in the plane of projection. The linking number $L(\alpha, \beta)$ of two orbits α and β is half the sum of their signed crossings.[6–9] The linking number of an orbit with itself (self-linking number) is defined as the sum (not half sum) of the signed crossings of the orbit with itself.[6–9] In Fig. 6, we illustrate such a procedure by determining the linking number of two ordered algorithm orbits.

Figure 7 shows the linking and self-linking numbers determined for a spectrum of ordered algorithm orbits corresponding to the IFS attractor reconstructed in Fig. 3. It has been shown that as the "wavelength" parameters $\omega_x = \omega_y$ are varied, IFS attractors can assume radically different symbolic dynamics.[1] A change in $\omega_x = \omega_y$ also yields a dramatic difference in the topological properties of the attractor. Figure 8 shows a partial embedding reconstruction of an IFS attractor identical to that in Figs. 1–3 except that $\omega_x = \omega_y = 0.80$. The linking numbers of a spectrum of ordered algorithm

	A	B	AA	AB	BA	BB	AAA	AAB	ABA	ABB	BAA	BAB	BBA	BBB
A	0	0	0	0	0	0	0	0	½	0	0	0	0	0
B		0	0	0	-½	0	0	1	-½	0	0	1	-½	0
AA			0	0	½	0	0	0	-½	0	0	0	½	0
AB				0	0	-1	0	0	0	1	0	-1	0	1
BA					0	-2	-½	0	-1	0	1	0	0	0
BB						1	0	0	0	1	0	0	-1	0
AAA							0	0	0	0	1	0	0	0
AAB								0	0	1	0	1	0	1
ABA									0	0	0	0	0	0
ABB										1	0	0	0	0
BAA											0	0	-½	0
BAB												0	0	0
BBA													0	0
BBB														1

Fig. 7 Spectrum of linking numbers of ordered orbits corresponding to the attractor reconstructed in Fig. 3.

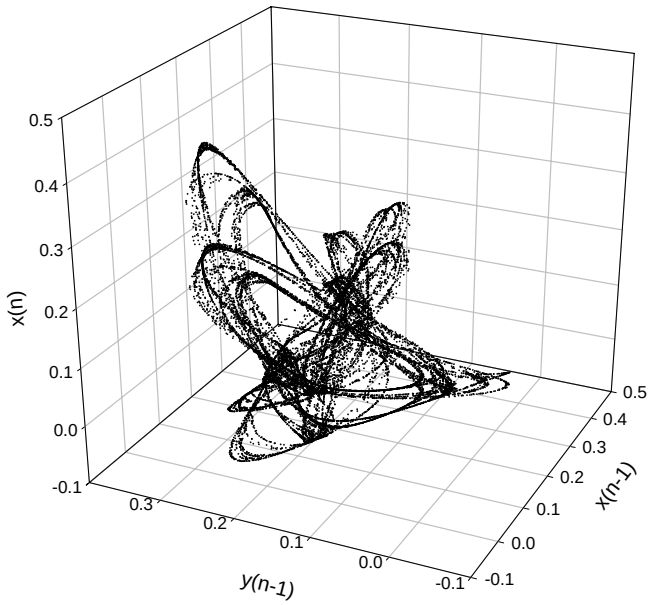

Fig. 8 Partial embedding reconstruction of an IFS attractor with parameters identical to those in Fig. 3, except that $\omega_x = \omega_y = 0.80$.

orbits corresponding to this attractor are shown in Fig. 9. Evidently, the topological structure is quite different from that illustrated in Fig. 7.

Time-delay embedding of IFS attractors and analysis of the reconstructed attractors using topological techniques provide an approach to characterizing the structure of these unusual attractors. However, many questions are raised by this approach. What is the significance of the ordered algorithm orbits? To what extent do their linking numbers actually describe the topology of IFS attractors? An infinite number of ordered algorithm orbits may be constructed; if a topological study were made of ordered orbits of increasing length, would some pattern emerge in the matrix of linking numbers? In what way (if any) does the topological structure of IFS attractors relate to their symbolic dynamics?

In classical chaotic attractors, the template of linking numbers is a topological invariant.[6] However, the templates shown in Figs. 7 and 9 are strongly dependent on the chosen embedding. For example, a template of linking numbers derived from orbits reconstructed in $x_{n-2}x_{n-1}x_n$ space shows much less topological connectivity than the partial embedding reconstructions considered here (in other words, in $x_{n-2}x_{n-1}x_n$ space, nearly all the linking numbers reduce to zero). The embedding dependence is not merely a characteristic of IFS attractor reconstructions; the reconstructed topology of at least one other nonlinear system has been shown to depend on the chosen time-delay embedding.[10] These and other issues will have to be addressed before we can fully assess what time-delay reconstructions can tell us about the structural and dynamical correspondence between IFS attractors and classical chaotic attractors.

	A	B	AA	AB	BA	BB	AAA	AAB	ABA	ABB	BAA	BAB	BBA	BBB
A	0	0	0	0	0	0	0	0	0	0	0	0	0	0
B		-1	0	0	0	-1	0	1	0	1	0	1	0	2
AA			0	0	0	-2	0	0	0	0	2	0	0	0
BA					0	-1	0	0	0	0	0	-1	1	0
BB						-1	0	1	0	0	0	0	0	0
AAA							0	0	0	0	1	0	0	0
AAB								0	0	1	0	0	0	0
ABA									0	0	0	0	0	0
ABB										1	0	0	0	0
BAA											0	0	0	0
BAB												0	0	0
BBA													0	0
BBB														1

Fig. 9 Spectrum of linking numbers of ordered orbits corresponding to the attractor reconstructed in Fig. 8.

REFERENCES

1. S. Bahar, "Symbolic Dynamics for IFS Attractors," *Fractals* **5**, 237–246 (1997).
2. M. F. Barnsley, "Fractals Everywhere," 2nd ed. (Academic Press, Inc., New York, 1993).
3. J. Stark, D. S. Broomhead, M. E. Davis and J. Huke, "Takens Embedding Theorems for Forced and Stochastic Systems," *Nonlinear Analysis — Theory, Methods and Applications* **30**, 5303–5314 (1997).
4. S. Bahar, "Orbits Embedded in IFS Attractors," *Int. J. Bifurcation and Chaos* **7**, 741–749 (1997).
5. S. Bahar, "Chaotic Attractors Generated by Iterated Function Systems: 'Harmonic Decompositions' and the Onset of Chaos," *Chaos, Solitons and Fractals* **8**, 303–312 (1997).
6. R. Gilmore, "Topological Analysis of Chaotic Dynamical Systems," *Rev. Mod. Phys.*, in press.
7. H. G. Solari and R. Gilmore, "Relative Rotation Rates for Driven Dynamical Systems," *Phys. Rev.* **A37**, 3096–3109 (1988).
8. G. B. Mindlin, X.-J. Hou, H. G. Solari, R. Gilmore and N. B. Tufillaro, "Classification of Strange Attractors by Integers," *Phys. Rev. Lett.* **64**, 2350–2353 (1990).
9. N. B. Tufillaro, H. G. Solari and R. Gilmore, "Relative Rotation Rates: Fingerprints for Strange Attractors," *Phys. Rev.* **A41**, 5717–5720 (1990).
10. G. B. Mindlin and H. G. Solari, "Topologically inequivalent embeddings," *Phys. Rev.* **E52**, 1497–1502 (1995).